Designing and Constructing an Animatronic Head Capable of Human Motion Programmed using Face-Tracking Software

A Graduate Capstone Project Report Submitted to the Faculty of the

WORCESTER POLYTECHNIC INSTITUTE

in partial fulfillment of the requirements for

the Degree of Master of Science

in Robotics Engineering

by Robert Fitzpatrick

Keywords:
1. Robotics
2. Animatronics
3. Face-Tracking
4. RAPU
5. Visual Show Automation

Primary Advisor
Sonia Chernova
Co-Advisor
Gregory Fisher

May 1, 2010

Table of Contents

Table of Figures

Table of Tables

Abstract

The focus of this project was to construct a humanoid animatronic head that had sufficient degrees of freedom to mimic human facial expression as well as human head movement and could be animated using face-tracking software to eliminate the amount of time spent on trial-and-error programming intrinsic in animatronics. As such, eight degrees of freedom were assigned to the robot: five in the face and three in the neck. From these degrees of freedom, the mechanics of the animatronic head were designed such that the neck and facial features could move with the same range and speed of a human being. Once the head was realized, various face-tracking software were utilized to analyze a pre-recorded video of a human actor and map the actors eye motion, eyebrow motion, mouth motion, and neck motion to the corresponding degrees of freedom on the robot. The corresponding values from the face-tracking software were then converted into required servomotor angles using MATLAB, which were then fed into Visual Show Automation to create a performance script that controls the motion and audio of the animatronic head during its performance.

Acknowledgements

I would like to thank everyone who helped me throughout my project, especially my advisors Sonia Chernova and Gregory Fischer, for their insight, support, and their patience. I would also like to thank Michael Allen at stereolithography.com for the quality parts that were produced for me, as well as how quickly they were produced. Lastly, I would like to thank my father, Edward Fitzpatrick, for the help he gave me in constructing the wooden electronics box and helping me arrive at the solution for the robot's spine, attaching the mechanics to the fiberglass shell.

1: Introduction

The animatronics industry is highly competitive and hires engineers and artisans that have both experience and expertise in their respective fields. This project is first and foremost an opportunity to gain experience in designing and constructing an animatronic head from the ground up. In addition to gaining experience within the scope of animatronics, this project also pursued the potential of programming animatronic had motions using facial and head tracking software. This is a technique that is relatively new in the industry, but it has not been used to its full potential. This researcher would not argue that the technology is used to its full potential in this project, but it was furthered in use compared to the current face-tracking methods used in the field. The current face-tracking methods, along with other applicable research efforts in animatronics are detailed in the following section.

1.1. Current Research in the Field

Hanson Robotics is one of the premier leaders of this industry. Their research into animatronics have lead to robots that can read faical expression, such as Zeno, and robots that can display and be controlled by an actor's facial expressions, Einstein and Jules (Hanson Robotics, 2009). The Hanson Robotics robots were all astounding in the realism they were able to portray with pliable skin and the number of actuators they had underneath that skin. However, due to the complexity of these robots, they serve best as models for inspiration than anything that useful information could be gained from for this project. Though, it is interesting to note that face-tracking and face-detection is being used on the more advanced animatronic robots in the industry.

Nexi, a robot designed by the MIT Media Lab, was designed to express human emotions while, unlike the Hanson Robotics robots, her face consists solely of moveable rigid components (Chandler, 2008). This robot is very similar to the end goal of the robot for this project. However, each eyebrow is individually controlled, as is each set of eyelids. This would over-complicate the robot in this project. It is something that is further addressed in the mechanical system section. Interestingly, though, Nexi has a rigid mouth that opens and closes, she has no horizontal control of her mouth to accentuate the movement of her lips to pronounce words. Though in Nexi's case, this does not seem all that necessary. This fact was useful in the design of the robot in this project.

1.2. Project Goals

The goal of this project is to design and build an animatronic head, then program it using data recorded from face-tracking software. The robot must meet the following requirements:

- The head must have the shape of a human's head
- The robot must have a human voice
- While the head will not have full functionality of a human head and face for simplicity, the features selected to be included must have the full range of an average human
- All movements must be recorded using face tracking software, where feasible
- The final animatronic head must have the capability to perform for a minimum of two minutes

2: Mechanical System

During the design process, two design spirals were performed. The first spiral created a preliminary design for the robot based upon both for the average human range of motion for each degree of freedom. Additionally, servo motors that were equal to or larger than the size of the motors that were to be designed in the second spiral, in order to insure that there was space available within the outer shell of the head such that all of the necessary components could fit inside.

In the second spiral, the design achieved in the first spiral was used to spec the servo motors that were used in the final product. The range of speeds achieved in each degree of freedom was also used to spec the servo motors. Additionally, the design achieved through the first spiral was fine tuned to fit the new motors that were purchased and to eliminate collisions of components while in motion.

2.1. First Design Spiral

2.1.1. Mannequin Decision

From the start, it was decided to purchase a premade mannequin head and then work from measurements obtained from it to create the mechanics of the robot. At first, it seemed like it would be easiest to work with a polystyrene head because it was light, inexpensive and easy to dismantle. Figure 1 below shows the polystyrene head that was purchased:

Figure 1: Polystyrene Mannequin Head

However, upon receiving the polystyrene head, it was clear that this head would not lead to an interesting character. Because of this, another option was pursued. The fiberglass bust in Figure 2 was the perfect fit in terms of character and aesthetics.

Figure 2: Mannequin Head with Character

This bust has features that had potential to lead to a successful character. After deeming this head acceptable for this project, the next step was to generate a conceptual image for look of the final product. Figure 3 depicts the final result for the conceptual image.

Figure 3: Final Product Concept Image

The overall appearance is intended to mimic that of a wooden ventriloquist dummy. The intent is to avoid the Uncanny Valley.

2.1.2. Mechanism Movement Constraints

The first step was to decide on the number of degrees of freedom. The rigid fiberglass shell eliminates all complexities that are inherent with the pliable skins used in the Hanson Robotics robots to mimic all facial movements. Even though the Nexi robot uses a large number of actuators to perform human emotions, the basic movements are both eyes pitching and yawing, eyelids opening and closing, each eyebrow translating and rotating, the mouth opening and closing, and the neck rolling, pitching, and yawing.

These movements can flow directly into discrete degrees of freedom. The eye yaw and pitch are controlled by two actuators respectively, for both eyes since human eyes always move in unison. The eyelids are controlled by one actuator since, in most cases, the eyelids move in unison, the exception being during the wink of one set of eyelids. The eyebrows were decided to be coupled together from the start such that there was only one actuator to control both eyebrows rotationally and translationally, this makes raising one eyebrow impossible, but this was acceptable to avoid overall complexity of the robot. The mouth corresponds to one actuator which opens and closes it. Lastly, the neck roll, pitch and yaw each correspond to an actuator in the neck. In total, the system was simplified down to have eight degrees of freedom, two in the eyes, one in the eyelids, eyebrows, and mouth and three in the neck.

Below is the data I have collected on average human facial and neck motions and speeds as well as the sizes of the corresponding body parts (where applicable). This data served as a foundation for this project, and was used to decide on the movement and size (where applicable) of the respective robot components. If data was unavailable, the measurements were performed on the researcher to find his average range of motion and speed.

2.1.2.1. Neck Motion

According to Kristi Stevens (2011) from Livestrong, the average human head can:

- roll (tilt left and right) 45° from the vertical, both the left and right
- pitch (tilt forward and back) 50° forward and 57.5° back
- yaw (rotate left and right) 70° from looking straight ahead, both left and right

Additionally, Victoria Quesada (2009) states that the head attaches to the spine at the atlanto-occipital joint at the end of the spinal cord. She continues to say that the head pivots on that joint when the neck moves and not halfway down the neck, like most people assume. Figure 4, from her blog, depicts the atlanto-occipital joint.

The researcher measured the speeds for the neck to roll, pitch, and yaw from one extreme to the other. The following maximum speeds were measured for each degree of freedom: 360 deg/s for roll, 430 deg/s for pitch, and 467 deg/s for yaw.

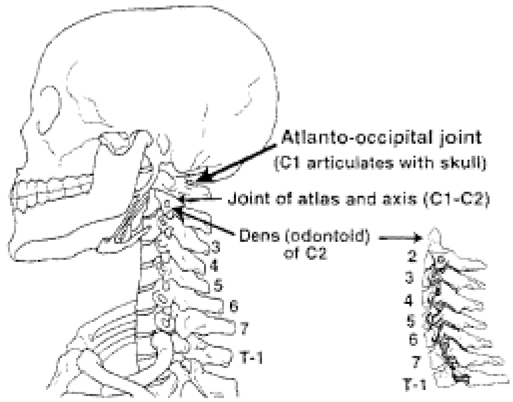

Figure 4: Atlanto-occipital Joint (Quesada, 2009)

2.1.2.2. Eyebrows

Jung and Sclafini (2010) present data that the eyebrow moves a total of 13 mm from the down (angry) to the up (surprised) positions. The rotational data, though not available in the research, was obtained through measurements performed by the researcher. In Figure 5, the down, neutral, and up eyebrow positions are shown, respectively.

Figure 5: Researcher's Eyebrow Angle Range

The angle measurements were found to be 29° for the down position, 8° for the neutral position, and 26° for the up position. Also measured was the linear speed of the researcher's eyebrow from the down to the up positions during its fastest motion. This speed was found to be 87 mm/s.

2.1.2.3. Eyes

According to Encyclopedia Britannica Macropedia (Sensory Reception, 1997), the average eye is 24 mm in diameter. Lefohn, Caruso, Reinhard, and Budge(2003) add that the average human iris is 12 mm in diameter, and Suzanne Robin (2011) from Livestrong states that the average human pupil has a radius of 2.5 mm. Tamler, Marg, Jamplonsky, and Nawratzki (1959) performed a study on saccadic eye movements, the fastest motion achieved by the human eye, and found that their highest measured mean angular velocity was 569.3 degrees per second.

The range of the motion could not be found in research, so it had to be obtained through measurements conducted by the researcher. Figure 6 below depicts the range of eye positions, and Figure 7 corresponds to the mapping of these moments onto the eyeball model to achieve measurements of the angular positions. No downward angle was easily achieved due to the tendency for the eyelids to close over the eye when looking down.

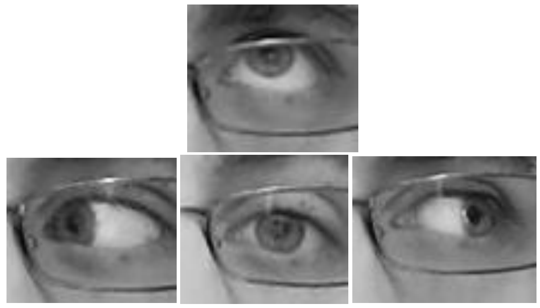

Figure 6: Researcher's Eye Range

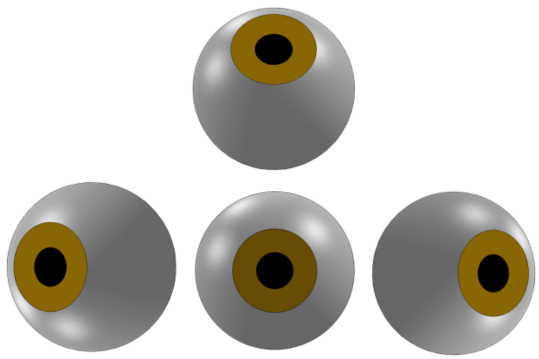

Figure 7: Corresponding Eye Orientations in CAD

The resulting measurements dictate that the eye has a fairly consistent range of 35° degrees of motion up, down, left and right.

2.1.2.4. Eyelids

The researcher measured angular motions of the eyelids since there was a lack of available information in the research. Figure 8 depicts the eyelid in the wide (surprised) state, the neutral state, and the closed state, respectively. Figure 9 corresponds to the mapping of these movements onto the eyelid models to achieve measurements of the angular positions.

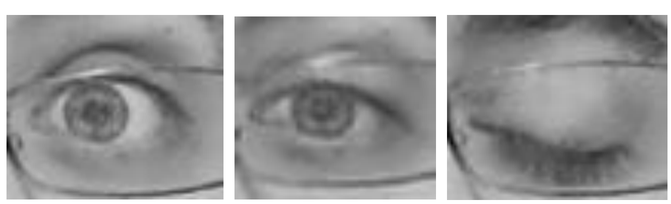

Figure 8: Researcher's Eyelid Range

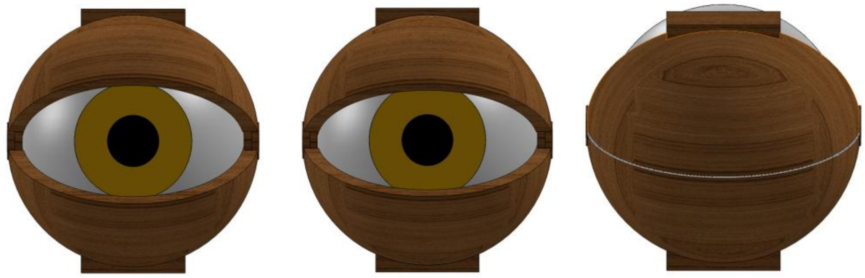

Figure 9: Corresponding Eyelid Orientations in CAD

The values are measured to be 30° from horizontal for both lids in the wide state, 26.8° from horizontal for both lids for the neutral state, and the bottom eyelid is 22° from the horizontal and the upper lid is in contact with the lower lid for the closed state. Even though there are multiple unaccredited resources online stating that it takes the human eyelid to complete one cycle of blinking over the course of 300 to 400 ms, this researcher performed a more exact study on the time it takes for this researcher's eyelids to close from the neutral state. The value was found to be an average of 173 ms for one half cycle of an eyelid blink, from neutral open to close. Since the top eyelid travels from 26.8° above horizontal to 22° below horizontal for one half cycle of an eyelid blink, this translates to a speed of 282 deg/s.

2.1.2.5. Mouth

Dijkstra, Hof, Stegenga, and De Bont (1999) present data that states the average distance a human can open their jaw is 57.2 mm. The measurements performed by the researcher show that the mouth can open at a maximum speed of 286 mm/s.

2.1.3. Neck Mechanism

The design process started with the neck mechanism—which needed to roll, pitch and yaw—since this dictated the location of the atlanto-occipital joint as well as the location at which the mounting plate for the rest of components would be located. Without knowledge of these two pieces of information, it would be difficult to design the rest of the robot.

The atlanto-occipital joint is a spherical joint, around which a human can roll, pitch, and yaw their head. This meant that it would be intelligent to model the neck mechanism as a spherical joint, which can be obtained through three rotational axes intersecting at perpendicular angles at a common, central point. This point is depicted as a red circle in Figure 10 below, also shown is the mechanism created to mimic a spherical joint. The neck mechanism was designed to ensure proper operation over the angular position range specified in section 2.1.2.1.

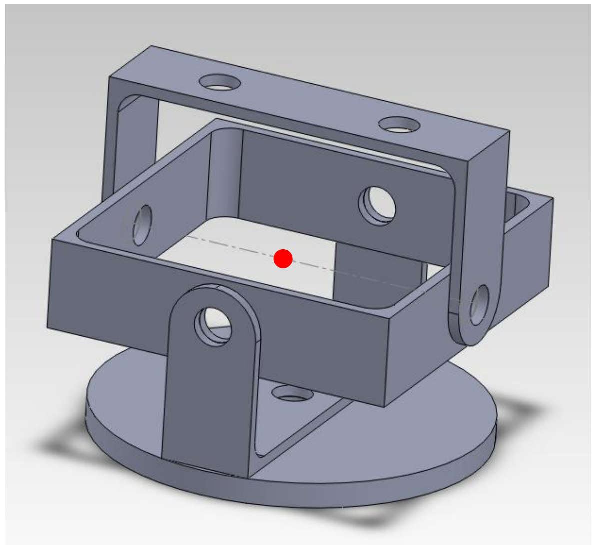

Figure 10: Neck Mechanism

The servo motors were positioned as shown in Figure 11 so that they would not collide with the fiberglass neck shell. However, since the motors were chosen to be oversized, the neck mechanism at this stage would not fit within the fiberglass shell, this was address in the second spiral during final servo motor selection.

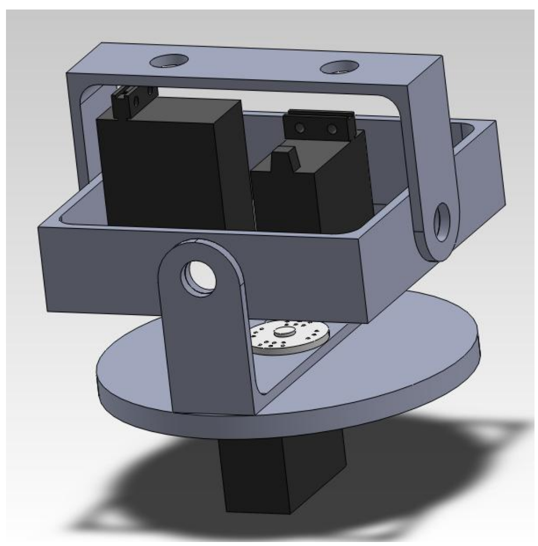

Figure 11: Original Neck Mechanism with Motors

2.1.4. Eyebrow Mechanism

The next mechanism to be designed was the eyebrow mechanism. The up, neutral, and down sates have are shown in Figure 12. Each state is represented by a solid gray line. The desired in-between states to reach each of the three states are represented as dotted gray lines. The vertical dotted line represents the constrained vertical motion the eyebrow must travel. All angles and linear motions match those called out in section 2.1.2.2.

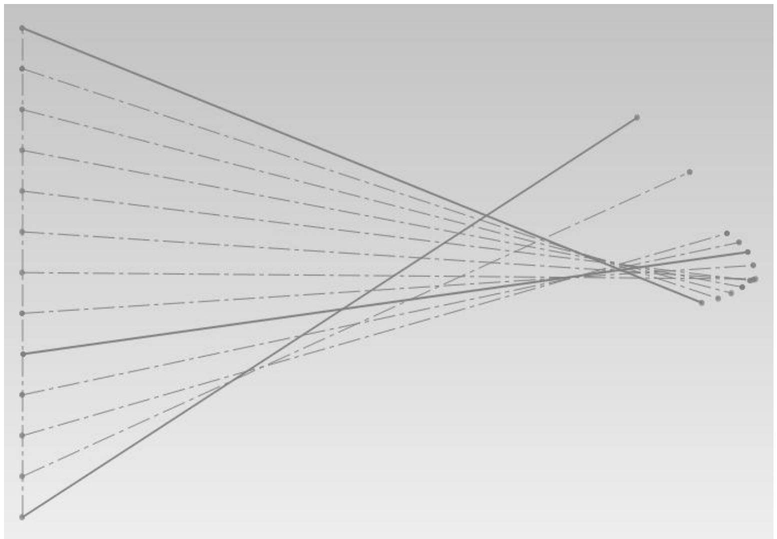

Figure 12: Eyebrow Motion

Each state line above represents the line parallel to the gray solid line superimposed over the eyebrow in Figure 13.

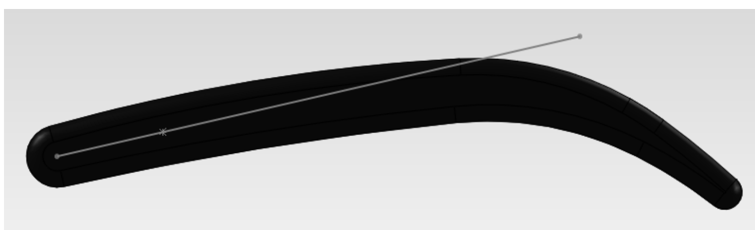

Figure 13: Corresponding Eyebrow Line

Using this motion plan, both translation and rotation were coupled together so that both eyebrows can be controlled by only one motor, as previously mentioned. First to be designed was the motion cam that would control the rotation of the eyebrow. Using the motion plan above, the cam below was designed. The solid black curve displays the path the eyebrow will travel.

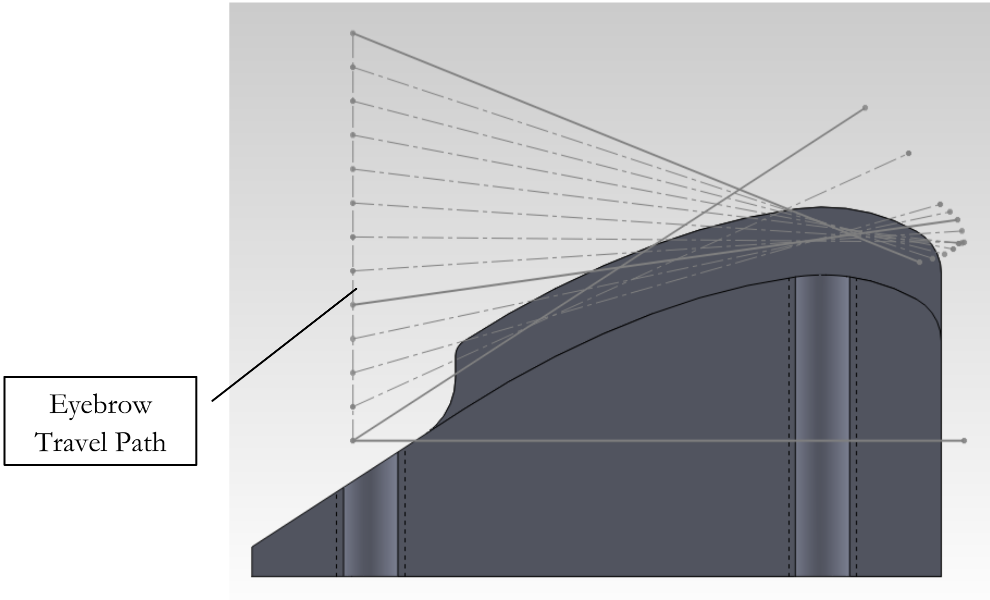

Figure 14: Eyebrow Cam Section View

Consequently, with this cam designed, the next step was to figure out how the eyebrow and the cam interacted. Figure 15 depicts the control rod that maps the cam motion to the eyebrow. Also included is the mounting plate that will attach the complete eyebrow mechanism to the rest of the head. Drawn in are springs that will keep the eyebrow control rod in contact with the cam at all times.

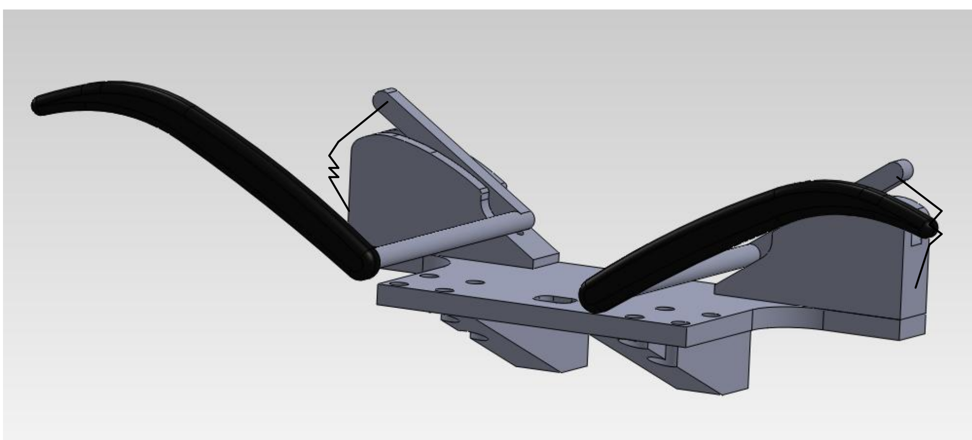

Figure 15: Mapping Cam Motion to the Eyebrows

Next, the method to control the vertical motion was designed. It was decided that the middle section of the eyebrow control rods would have vertical channels to travel along with stops on either end to prevent the eyebrow from traveling in outside of the desired range. A cross-section of the realized mechanism is shown in Figure 16.

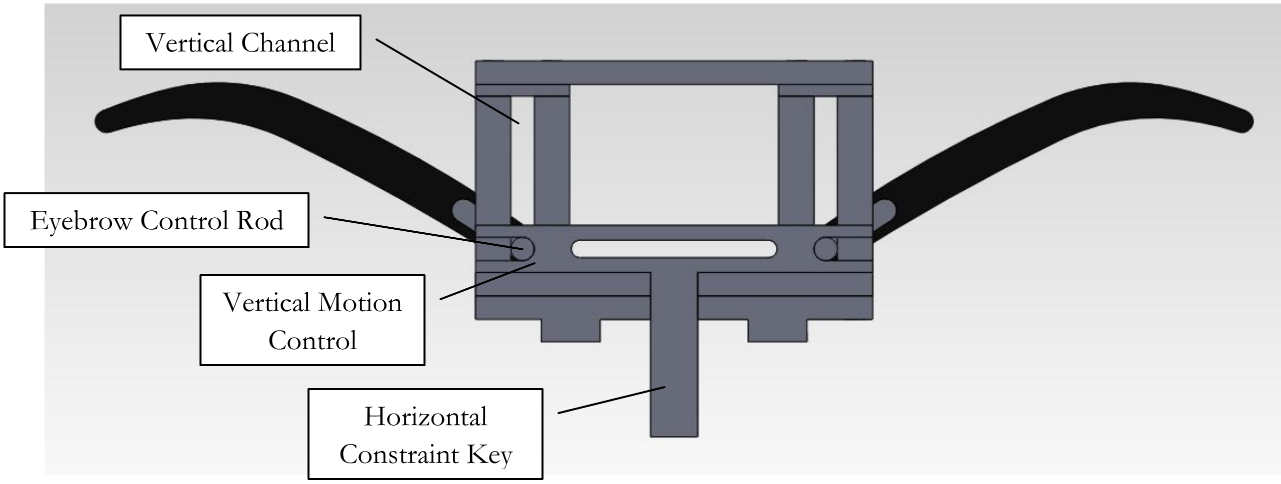

Figure 16: Eyebrow Vertical Control Mechanism

The vertical channel shown above is capped, as shown. The vertical motion control moves up and down, moving the eyebrow control rod up and down with it, while still allowing the eyebrow control rod to rotate as dictated by the cam. The key shown in the picture prevents the vertical motion control piece from rotating. The key maintains horizontal orientation throughout its range of motion. Figure 17 shows how the servo motor was attached to the eyebrow system.

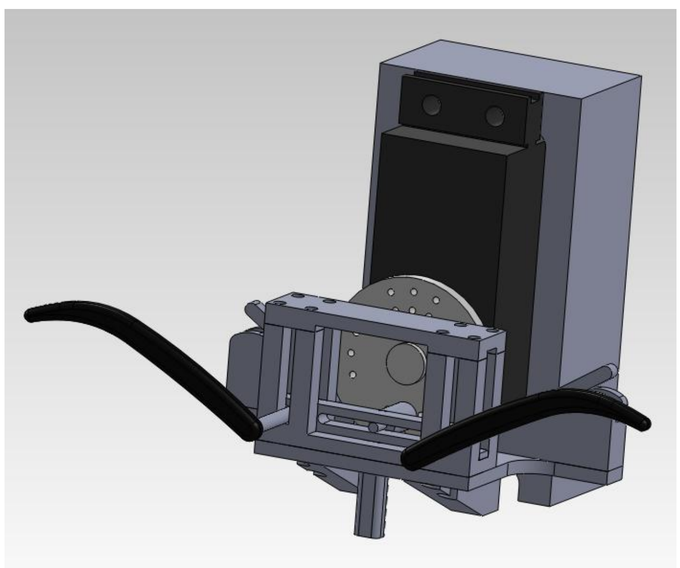

Figure 17: Complete Eyebrow Mechanism

2.1.5. Eye Mechanisms

The eye was designed to operate with a universal joint because of space limitations, since the outer diameter of the eye is only 24mm. A cross section of the eye assembly is shown in Figure 18.

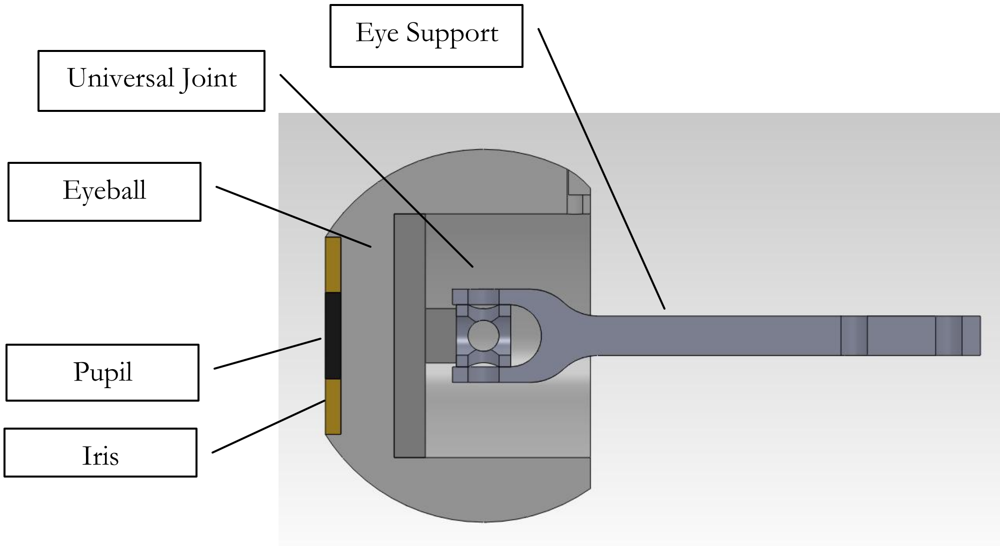

Figure 18: Eye Section View

The yaw and pitch and mechanisms used to control the eye movement about the pivot created by the universal joint are detailed in the following sections.

2.1.5.1. Eye Yaw Mechanism

In Figure 19 below, the motion required for the eye yaw mechanism, as prescribed in section 2.1.2.3, is drawn onto the top view of the robot thus far.

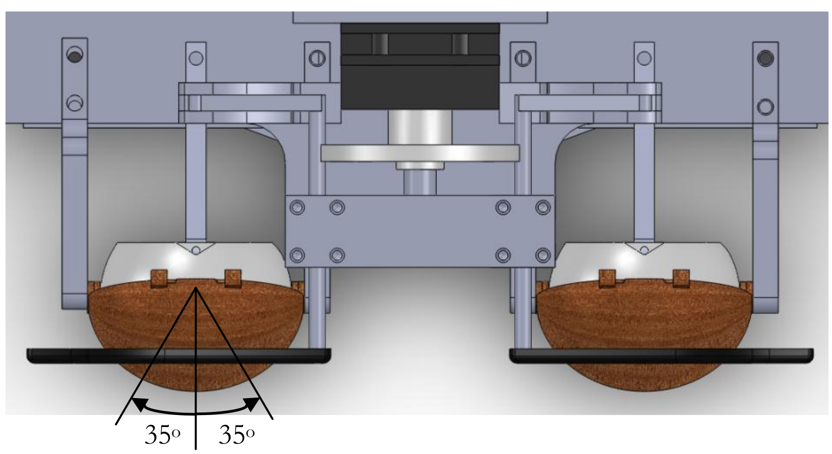

Figure 19: Eye Yaw Requirements

A parallel motion linkage was designed to address this required motion. Figure 20 depicts the input link that mimics the size and orientation of the eye, to incorporate parallel motion.

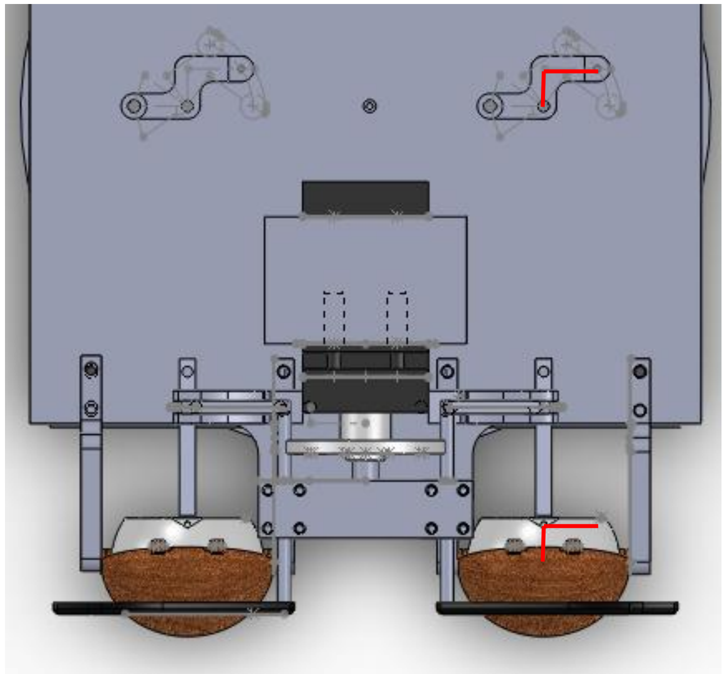

Figure 20: Input Link Mimicking the Output Link

The two sets of red lines start at their corresponding link's (either the eye or the input link) pivot point and travel vertically and right to the location to which the coupler link attaches. The pivot point and the point where the coupler attaches are exactly the same distance apart for both the input link and the output link (the eye). Next the coupler link was created so that it connected the input and output link. Figure 21 shows the resulting coupler link.

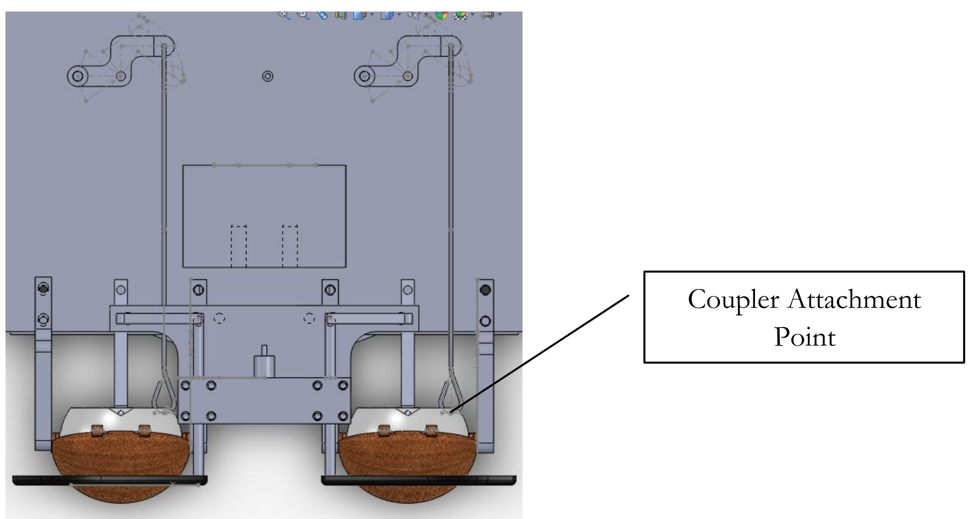

Figure 21: Eye Yaw Mechanism Coupler Link

The next step was to design a separate mechanism that can create identical motion between the left and right eye.

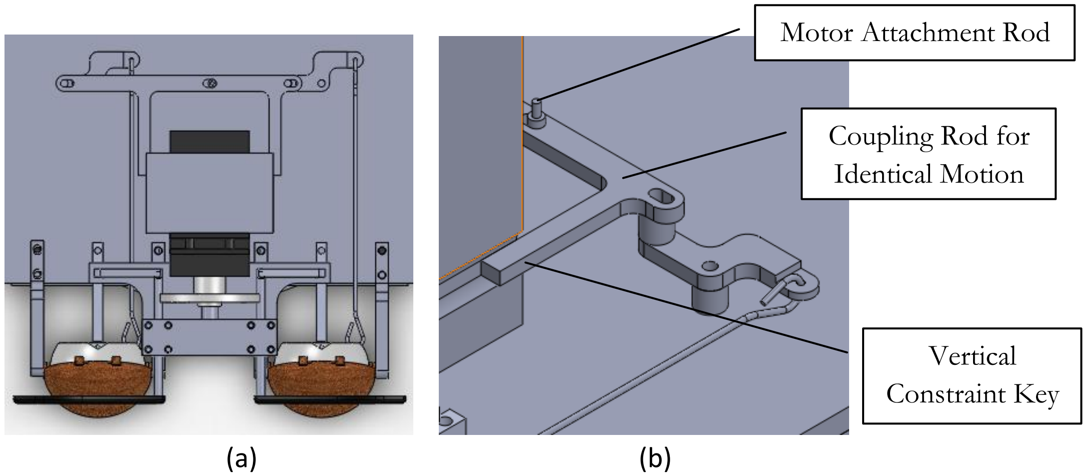

Figure 22: (a) Eye Yaw Control Linkage, (b) Detailed Side View

The vertical constraint key in Figure 22 keeps the coupling rod for identical motion from rotating. When the coupling rod for identical motion moves forward or backward, both eyes rotate right and left respectively. The motor attaches to the motor attachment rod shown in the picture and controls motion similar to the eyebrow motor by rotating. A view from the back is shown in Figure 23.

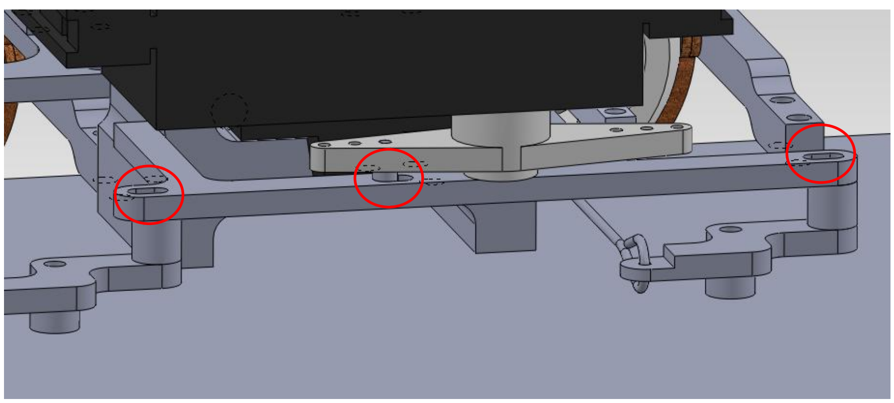

Figure 23: Back View of Eye Yaw Mechanism

The slots circled in red allow for the motor to rotate and for the two input links to rotate exactly 35° forward and exactly 35° back as the motor rotates. The robot thus far into the process is shown in Figure 24. It includes the initial robot, the eyebrow subassembly, and the eye yaw subassembly.

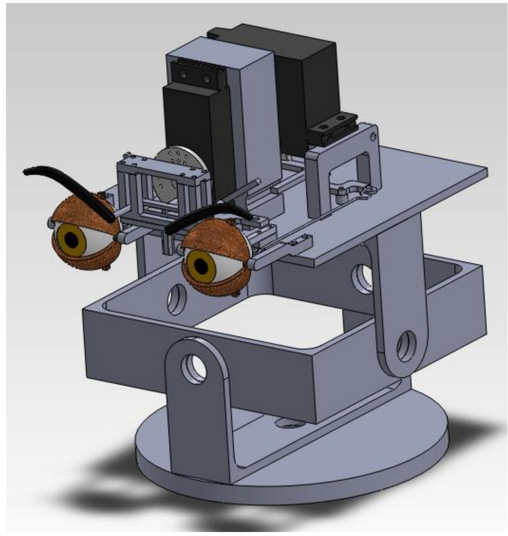

Figure 24: Initial Assembly with Eyebrow and Eye Yaw Subassemblies

2.1.5.2. Eye Pitch Mechanism

Drawn in Figure 25 is the motion required for the eye pitch mechanism as specified in section 2.1.2.3.

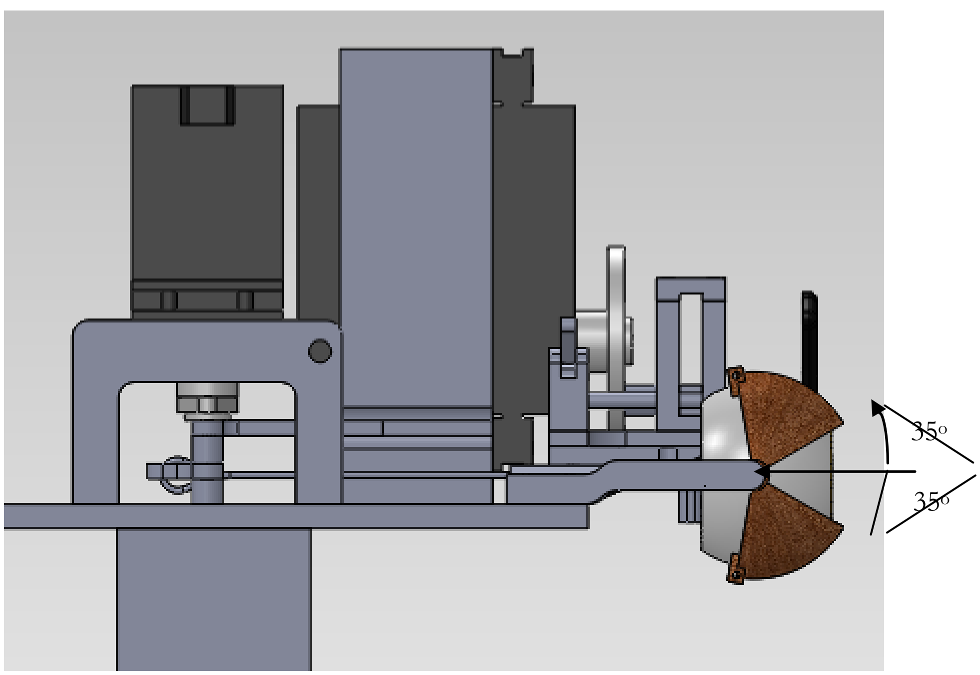

Figure 25: Eye Pitch Requirements

To address this required motion, another parallel motion linkage was deemed to be the best solution. Figure 26 depicts the input link that mimics the size and orientation of the eye.

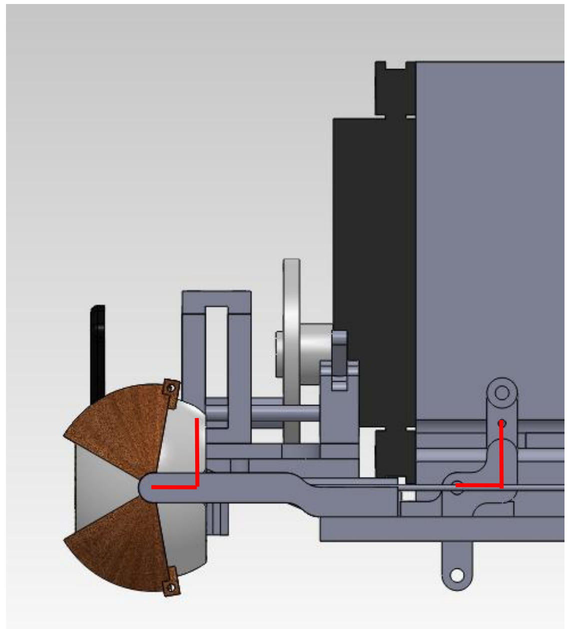

Figure 26: Input Link Mimicking the Output Link

The two sets of red lines start at their corresponding link's (either the eye or the input link) pivot point and travel vertically and right to the location to which the coupler link attaches. The pivot point and the point where the coupler attaches are exactly the same distance apart for both the input link and the output link (the eye). Next the coupler link was created so that it connected the input and output link. Figure 27 shows the resulting coupler link.

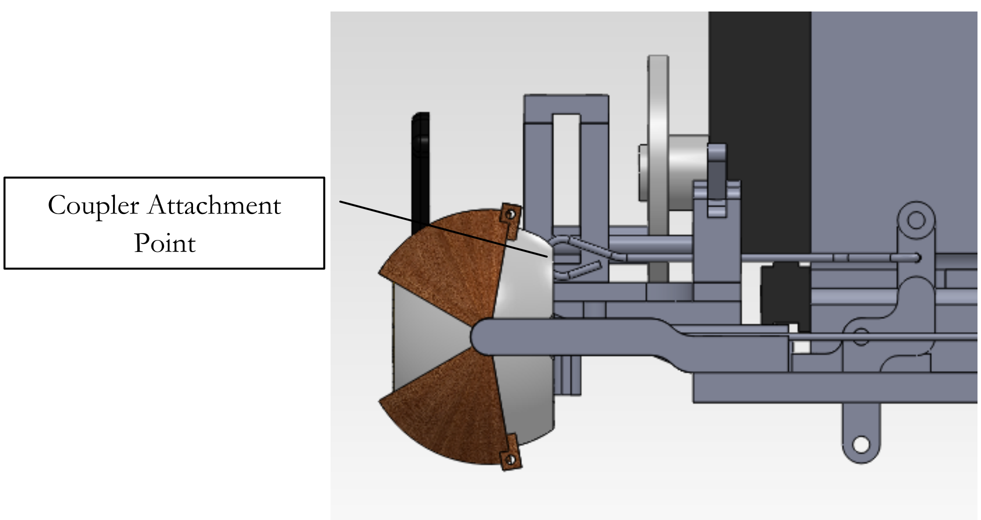

Figure 27: Eye Yaw Mechanism Coupler Link

The next step was to create a link that creates identical motion between the left and right eye, shown in Figure 28.

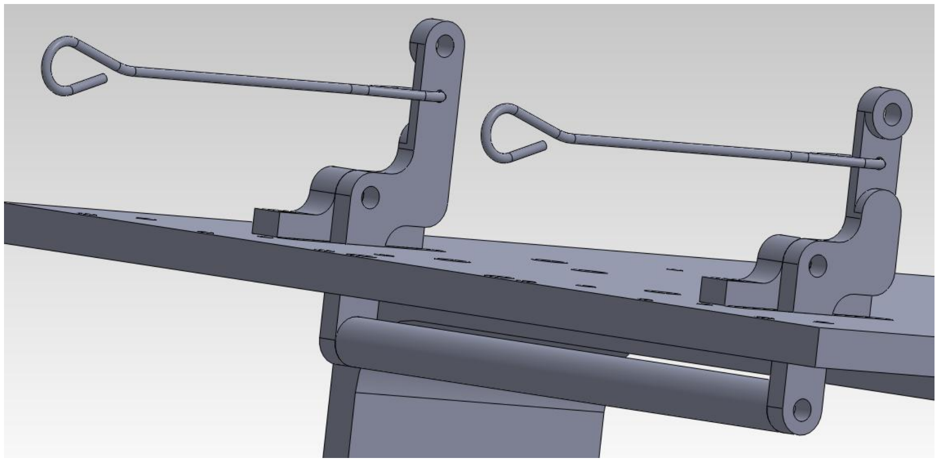

Figure 28: Eye Yaw Identical Motion Mechanism

The rod linking the right side to the left side forces the left and right eyes to move in sync. The next step was to figure out how to control the motion of pitch of the eyes using a motor. Figure 29 and Figure 30 below depict the resulting linkage and the analysis phase that led to the decision.

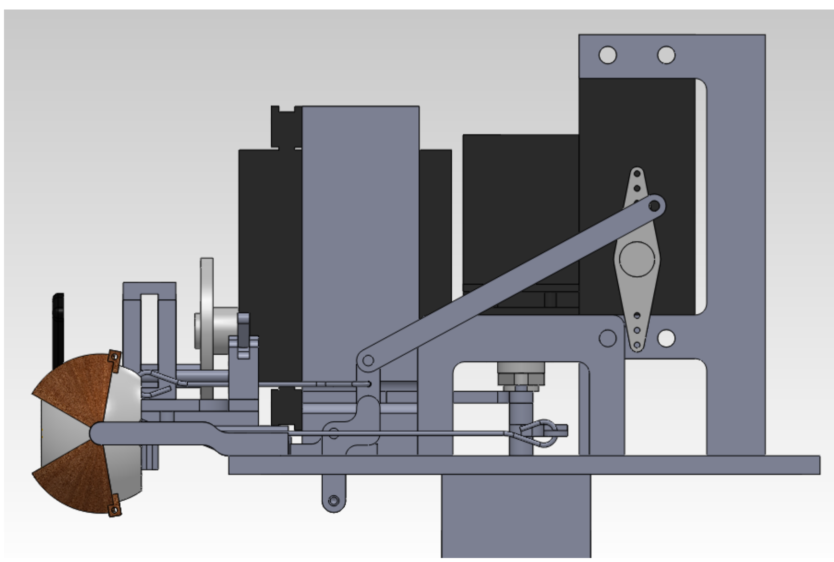

Figure 29: Side View of Eye Pitch Mechanism

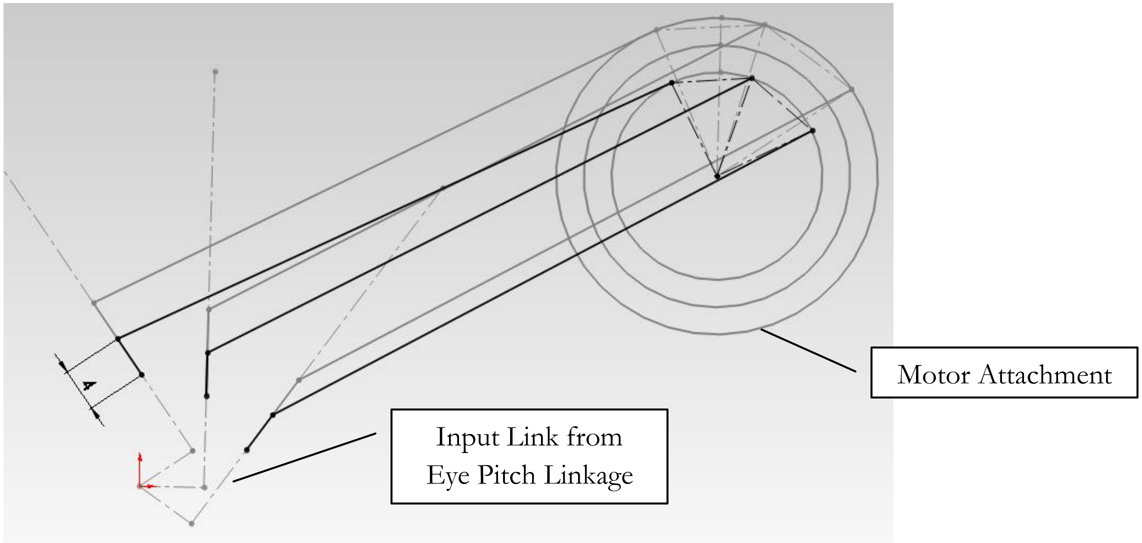

Figure 30: Eye Pitch Mechanism Plan

The black lines in the last image represent the potential linkage that could connect the motor to the input linkage of the eye pitch linkage. The solid gray lines represent the portions of the assembly that are stationary, such as the rotation and link of the input link from the eye pitch linkage and the position and diameter of the motor and the servo horn. Below is the robot thus far into the process in Figure 31. It includes the initial robot, the eyebrow subassembly, the eye yaw subassembly, and the eye pitch subassembly.

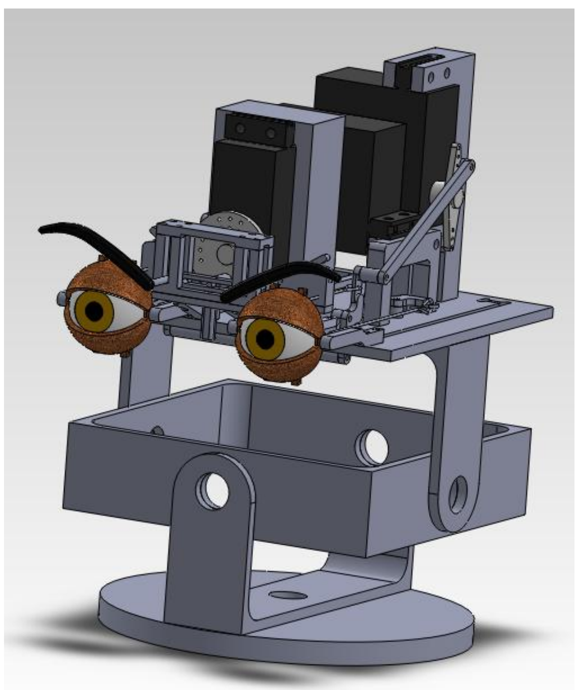

Figure 31: Initial Assembly with Eyebrow, Eye Yaw, and Eye Pitch Subassemblies

2.1.6. Eyelid Mechanism

Based on the study of how my eyelids operate in section 2.1.2.4, Figure 32 depicts the wide, open, and closed states, with green representing the wide open eyelids, yellow representing neutrally open eyelids, and red representing the closed eyelids.

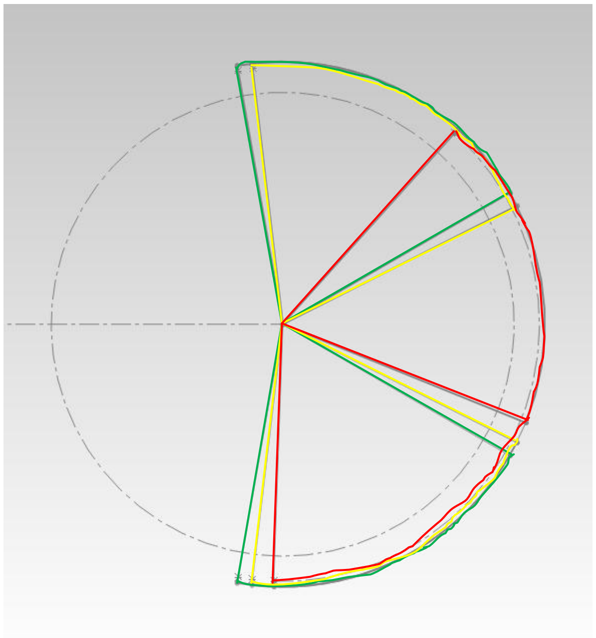

Figure 32: Eyelids Wide Open, Relaxed Open, and Closed

The next step was to design a linkage and motor system that could open and close the eyelids. Below is the sketch that was used to create the eyelid linkage. The linkage outlined in red is the position of the linkage with the eyelids closed.

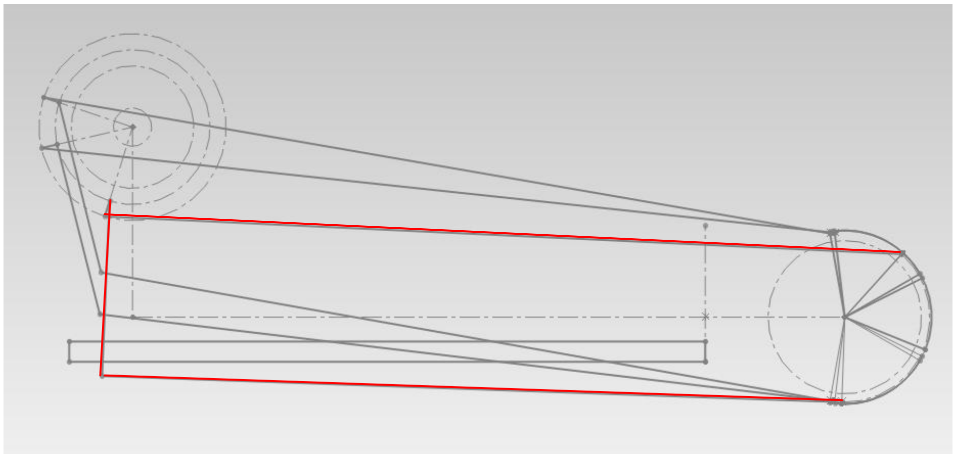

Figure 33: Eyelid Linkage Plans

The eyelid linkage was then modeled for the right side of the head and is depicted in Figure 34 below.

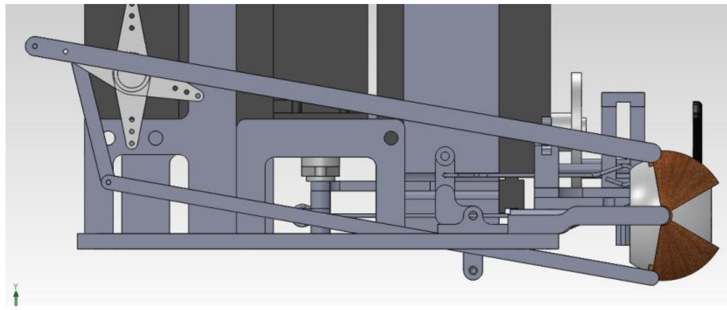

Figure 34: Eyelid Linkage

The right side was then connected to the left side eyelids so that they could open and close in sync. Figure 35 below shows the solution in a top and left side view.

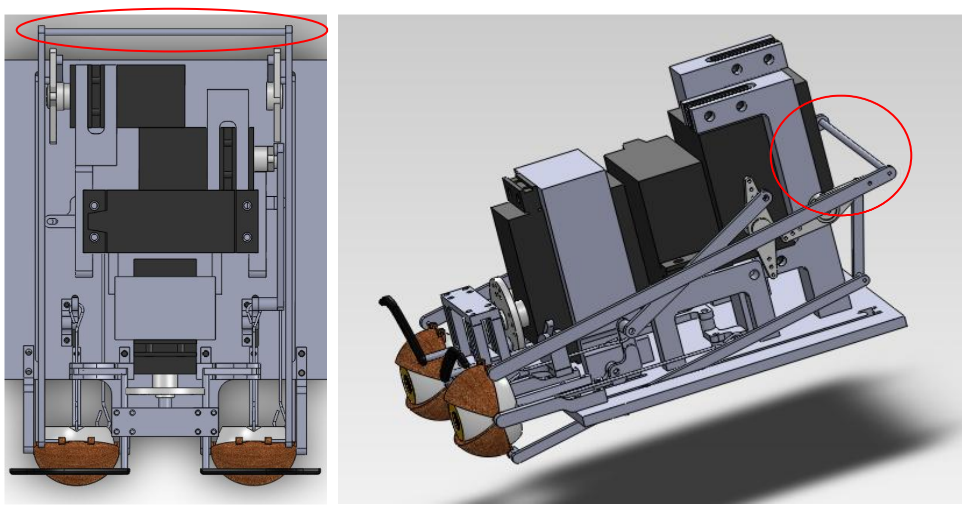

Figure 35: Linking Right Eyelid Linkage to Left Eyelid Control

This solution is not the best one because of the large amount of torque and cantilevering that the solution will experience, however with the limited space available, the solution is the best available. The robot as it is thus far into the process is depicted below in Figure 36.

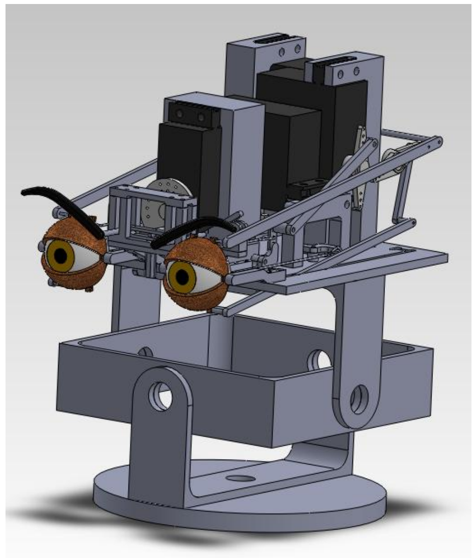

Figure 36: Assembly with Eyebrow, Eye Yaw, Eye Pitch, and Eyelid Subassemblies

2.1.7. Jaw Mechanism

The jaw mechanism was the simplest mechanism to design, since the mouth only needs to rotate around a fixed point, the same way a human jaw does. Additionally, the only states needed were opened and closed. Figure 37 below depicts the plans for the mouth mechanism. Green represents the jaw opened and red represents the jaw closed. Orange depicts the coupler link that attaches the output link (the jaw) to the motor.

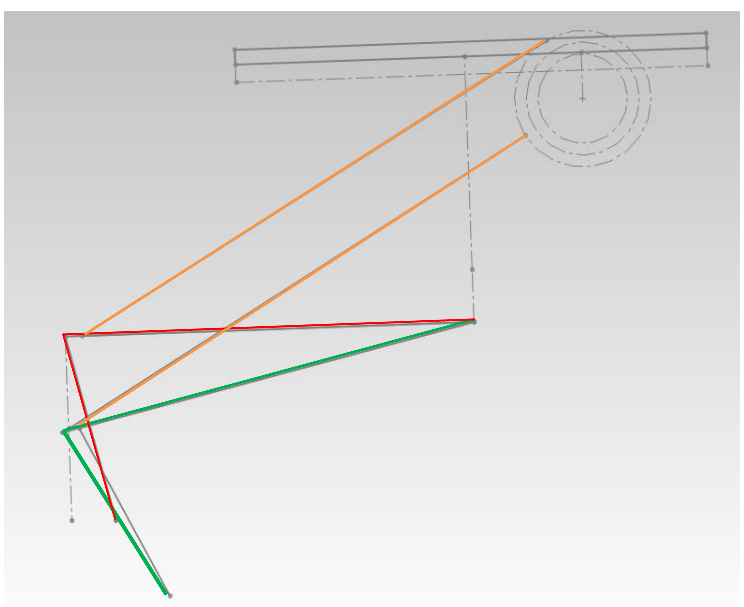

Figure 37: Jaw Mechanism Plans

These plans were then transitioned into physical parts, which are shown in Figure 38. Also in the image is the motor that actuates the jaw.

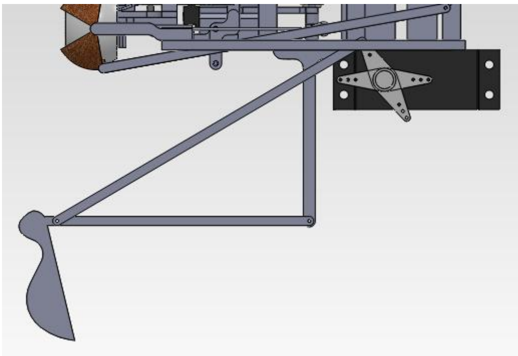

Figure 38: Jaw Linkage

Below in Figure 39 is the robot thus far into the process. It includes the final version of the first spiral robot (without the neck mechanism for clear illustrational purposes). Included in the figure are the eyebrow subassembly, the eye yaw subassembly, the eye pitch subassembly, the eyelid subassembly, and the jaw subassembly.

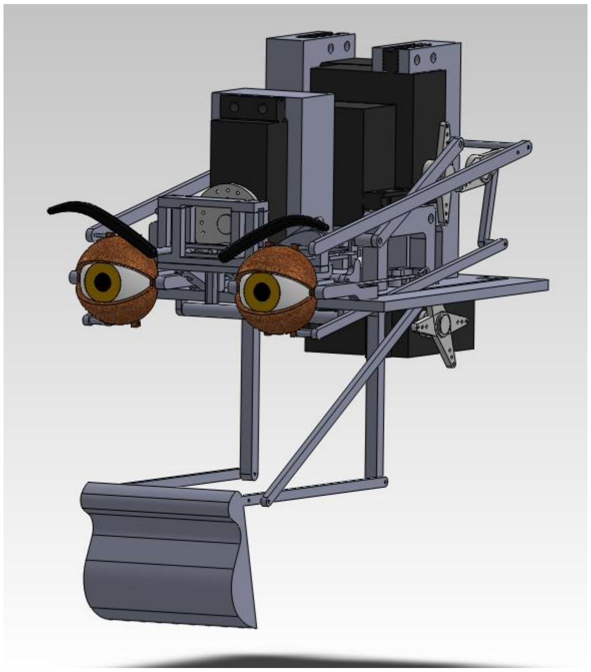

Figure 39: Assembly with Eyebrow, Eye Yaw, Eye Pitch, Eyelid, and Jaw Subassemblies

2.2. Second Design Spiral

The second design spiral the design achieved in the first spiral was redesigned to such that the servo motors decided on in the following section would fit better within their assemblies. Additionally, collisions were removed by redesigning components in each assembly.

2.2.1. Servo Motor Selection

The measured speeds specified in sections 2.1.2.1 through 2.1.2.5 were used to determine the servo motors used for each degree of freedom. Using the kinematic relationship of the input link speeds to the output link speeds in each linkage, the necessary speeds of each motor can be obtained. Table 1 presents the output link speeds provided in the first spiral section, along with the motor speeds needed to create those output link speeds, as well as the motor speed specification (s/60°) needed to pick each servo motor.

DOF	Output Link Speed	Motor Speed (deg/s)	Motor Speed (s/60°)
Neck Roll	360 deg/s	360	0.17
Neck Pitch	430 deg/s	430	0.14
Neck Yaw	467 deg/s	467	0.13
Eyebrows	87 mm/s	200	0.30
Eye Pitch	569.3 deg/s	667	0.090
Eye Yaw	569.3 deg/s	835	0.072
Eyelids	282 deg/s	357	0.168
Jaw	286 mm/s	300	0.20

Table 1: Servo Motor Speeds Obtained From Output Link Speeds

Since the neck roll, pitch, and yaw motors are directly attached to the outputs, the angular speeds are the same. The values in the fourth column, motor speed in s/60°, are a conversion of the third column from deg/s to s/60° (which translates to the time it takes the servo to rotate 60°) since servo motor speeds are based on the latter unit.

The torques required for each motor are calculated based on the first spiral design with each non-servo-motor component made from SLA. This is the material that was decided on for the final assembly since it is light, quick to manufacture, and relatively inexpensive. Table 2 below depicts twice the value of the calculated torques needed for each degree of freedom. It is important to note that the torques have been doubled to account for added torques that will be caused by friction.

DOF	Torque (kg-cm)
Neck Roll	6.481
Neck Pitch	5.245
Neck Yaw	7.851
Eyebrows	0.100
Eye Pitch	0.102
Eye Yaw	0.150
Eyelids	0.117
Jaw	0.547

Table 2: Motor Torque Requirements

All specifications in the torque and speed tables are specified for servo motor operations at 6 volts. With this information in mind and based on the torques and speeds required for each degree of freedom, the following servo motors have been decided on. The neck roll and neck pitch were decided to be controlled with Hitec HS-7775MG servos, since they have a maximum torque of 9.0 kg-cm and a maximum speed of 0.10 s/60°. This motor is sufficient for both degrees of freedom and is desirable because it has a low profile and both servos could fit within the neck mechanism without any collisions with the links or the neck of the fiberglass bust. The HobbyKing HK47011DMG was decided on for the neck yaw motor since it has a maximum torque of 10.80 kg-cm and a maximum speed of 0.07 s/60°. This motor has sufficient torque to rotate the entire head assembly. The Hitec HSG-5084MG was decided on for the eyebrows, eye pitch, eye yaw, eyelids, and jaw servo motors because the motor has a torque of 1.87 kg-cm and a speed of 0.05 sec/60°. Both of these values met the requirements for each of the five degrees of freedom, plus there were few other servo motor options that supplied less torque while still meeting the requirements.

The motors were inserted into each of their respective assemblies, as shown in the following sections. Also detailed in the following sections are the changes to each of the assemblies that eliminate collisions, as previously mentioned, or simplify the assemblies overall.

2.2.2. Neck Mechanism

The second spiral led to a more sophisticated neck mechanism. Figure 40 depicts the mechanical hard stops that were added to prevent the links from rotating beyond their desired range of motion. The figure also depicts the ribs that were added to strengthen the rolling link as well as the base of the robot which was thickened to ensure that it was sturdy enough to support the robot during its motion and heavy enough to anchor the rest of the assemblies.

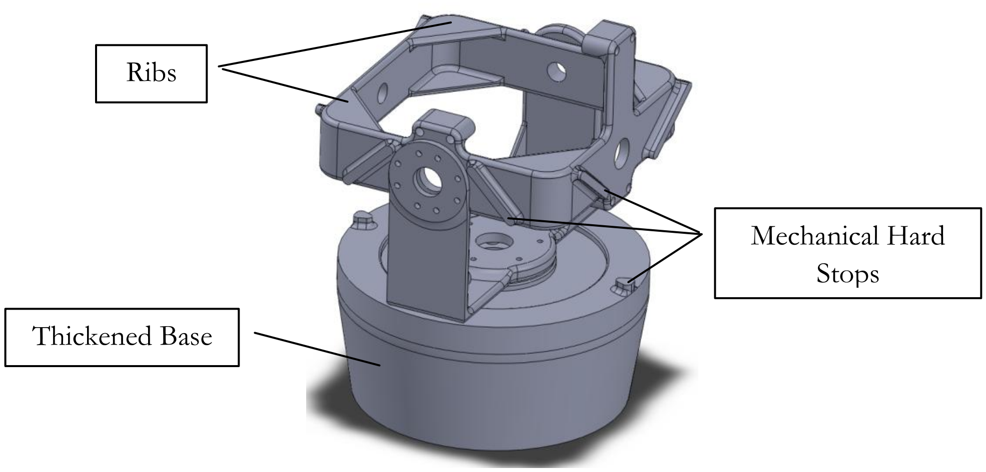

Figure 40: Second Spiral Sophisticated Neck Mechanism

The implementation of the HS-7775MG servo motors allowed for the overall sizes of the linkages to shrink, as previously mentioned. The neck mechanism now fit comfortably within the constraints of the fiberglass bust. It is important to note that the pitch link, which originally connected to the main attachment plate of the head, is not in the picture because it was incorporated into the main attachment plate of the head. Figure 41 below depicts the neck mechanism with the motors in place. The HK47011DMG, though not easily seen in the picture, is housed inside the base of the robot such that the servo horn rotating the yaw link of the mechanism.

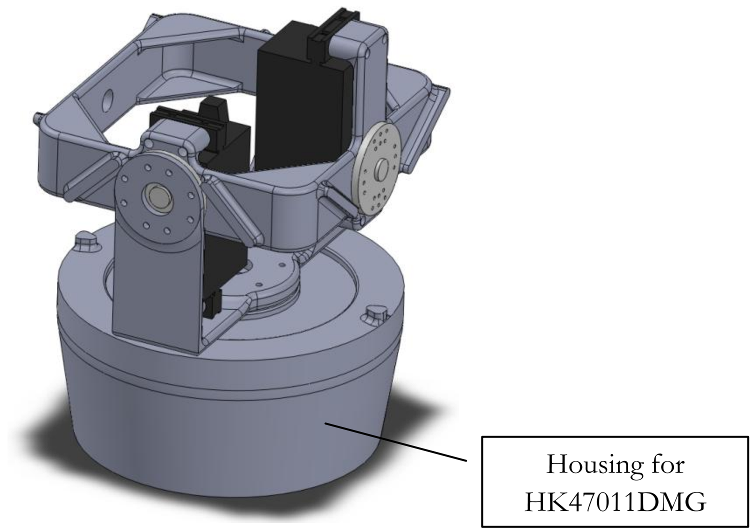

Figure 41: Spiral Two Neck Mechanism with Motors

2.2.3. Eyebrow Mechanism

The second spiral simplified the overall part count of the eyebrow mechanism. Though there were no collisions to eliminate, the parts that did not need to be separate from each other were combined to decrease the overall part count. The second spiral assembly is shown in Figure 42.

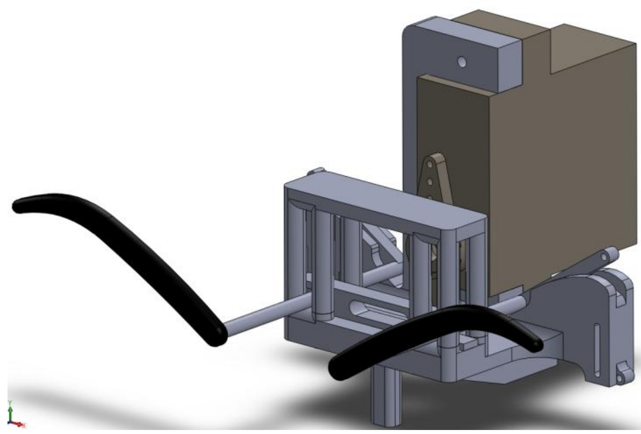

Figure 42: Second Spiral Eyebrow Assembly

The implementation of the HSG-5084 MG allowed for the original motor attachment to shrink in size and attach directly to the mounting plate from the original design, the eyebrow control cams were also attached to the plate. The parts maintaining vertical motion of the eyebrow control rods were combined such that they consisted of only two components, the mounting plate and the part consisting of the vertical channels.

2.2.4. Eye Mechanisms

Three changes affected both the eye yaw and eye pitch mechanisms. First, the eyeball was redesigned such that the coupler links could slide along the surface that the coupler link pulls on to move the eye. This was done because the original design did not account for the rotational motion of the attachment position, which is created because the attachment method is not on a point horizontally or vertically collinear with the pivot point of the universal joint. This change to the eyeball is shown below in Figure 43.

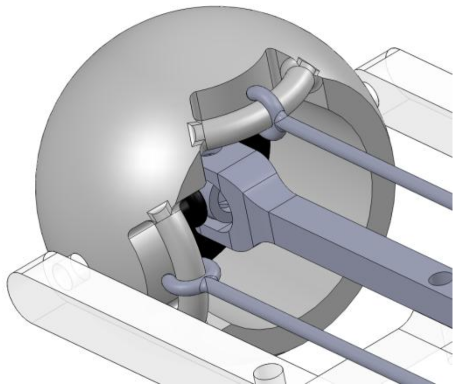

Figure 43: Second Spiral Coupler Attachment Method to Eyeball

This changed attachment method allowed the pitch coupler rod to remain parallel to the top and right planes as the yaw coupler rod is operating, and vice versa. Both control rods can be moved at the same time, as well, while the control rods consistently remain parallel to each other and the top and right planes of the overall assembly.

The second change, which is related to the first change, is that the control rod design was changed so that it could be manufactured out of SLA, instead of bent wire like originally intended. This change allowed it to snap easily into place and be precise in its motion, when the design in the first spiral was not precise while it was moving. This change is shown in both Figure 43 and Figure 44.

The third change was made to the input links at the other end of the coupler links. Below, in Figure 44, is a cross-section of the second spiral concept, where the coupler link snaps directly to the post positioned inside of a cylindrical slot in the input link. The geometry of the slot allows the coupler link to rotate without restriction for the entire range of motion of the eyeball. The pitch input link is shown in the image, but the same design idea was implemented on the yaw input link as well.

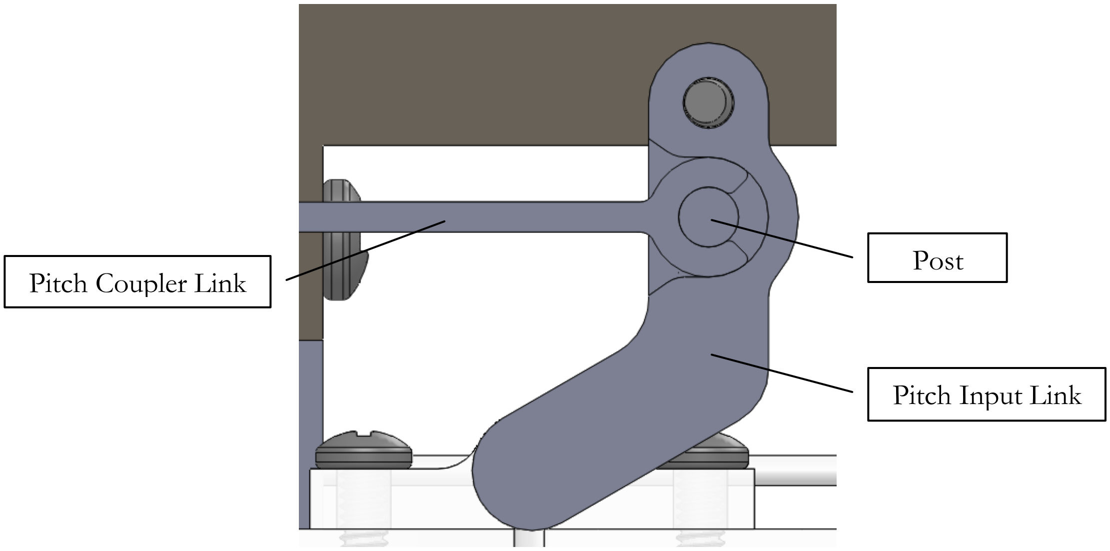

Figure 44: Second Spiral Coupler Attachment Method to Input Link

2.2.4.1. Eye Yaw Mechanism

The second spiral yaw mechanism is shown in Figure 45 below. The only change, outside of those mentioned above, was that the vertical constraint key had to be redesigned since the eyebrow motor mount was no longer available to act as the keyway. The keyway was instead designed into the motor mount.

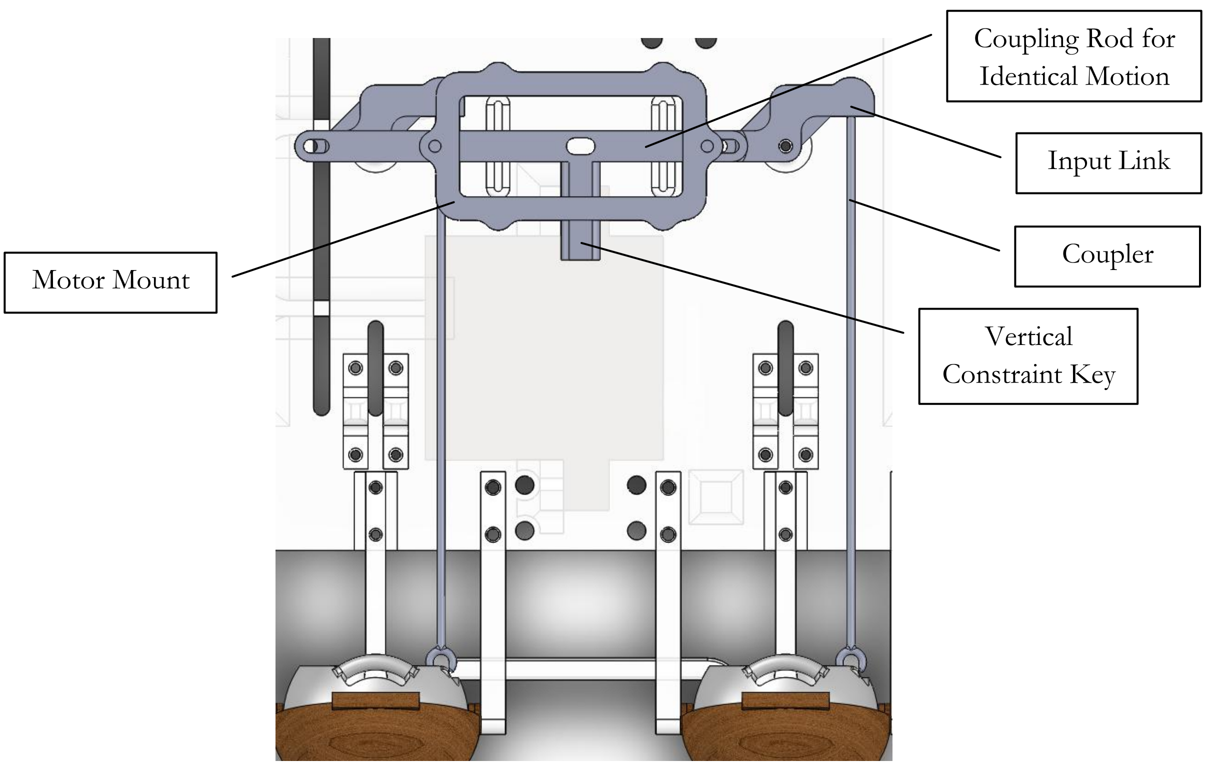

Figure 45: Second Spiral Yaw Mechanism

2.2.4.2. Eye Pitch Mechanism

Apart from the motor being added and the motor mount being resized and the changes already mentioned, there was only one discernible change. The rod connecting the left side to the right side was moved above the main attachment plate of the head since it allowed for both the input links and the connecting rod to be combined into one part. Also, it allowed for the jaw motor to be relocated to the front of the head to eliminate the collisions the jaw had with the neck in the first spiral. The change is shown below in Figure 46.

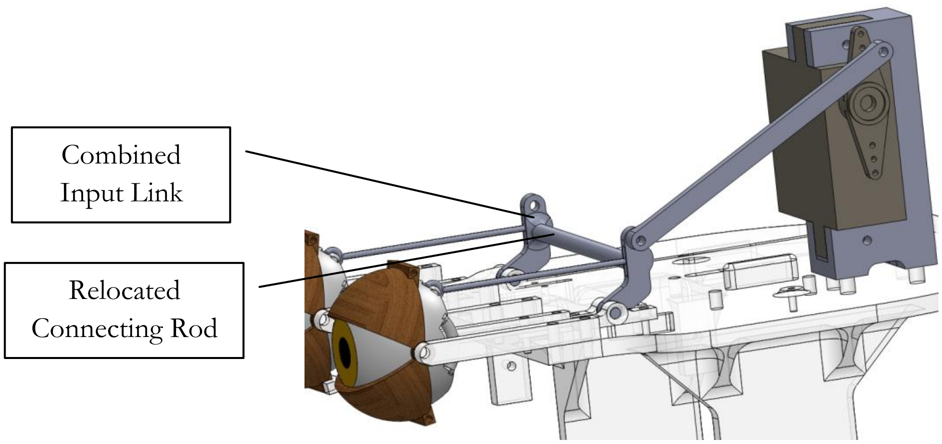

Figure 46: Second Spiral Pitch Mechanism

2.2.5. Eyelid Mechanism

There were only two changes made to the eyelid mechanism in the second design spiral. The coupler links for the top eyelids were connected, just as the input links in the spiral pitch mechanism were. The connecting rod was joined with both the left and right side coupler links for the top eyelids. The second change was that the bottom two eyelids were joined using a separate joining rod. This rod was not combined with the bottom eyelids only to ensure part uniformity across all four eyelids. The changes are shown in Figure 47 below.

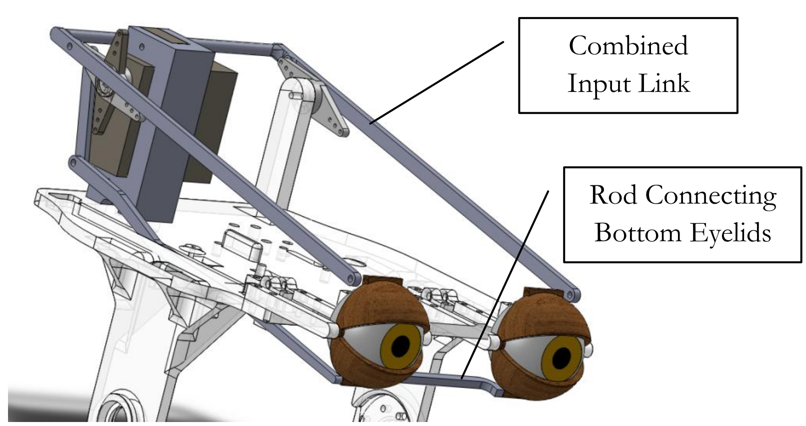

Figure 47: Second Spiral Eyelid Mechanism

2.2.6. Jaw Mechanism

The jaw mechanism was the only subassembly that was almost completely redesigned during the second spiral. The jaw mechanism had the most collisions, so it was in need of a reassessment. To address the issue of the jaw colliding with the neck mechanism and the motors within it, the jaw servo motor needed to be moved towards the front of the head. Moving the motor forced the need to redesign the jaw linkage such that the desired motion could still be achieved. This led to the repositioning of the output link pivots to be collinear with the neck pitch pivots, since the jaw and the neck pivot are nearly coincident on the human head. Moving the jaw output pivot to the outside of the neck pitch pivot eliminated most collision issues that were found in the first design spiral.

The output link was designed to have attachment methods similar to the coupler links in the eye subassemblies, such that they could simply clip onto the neck pitch linkage, which was attached the main attachment plate of the head as previously mentioned. The attachment posts in this case, however, needed to be stylized like the inverse of a half torus since bolts that acted as pivot axes for the neck pitch linkage needed to be attached in the centers of each post. The second spiral jaw mechanism is shown below in Figure 48.

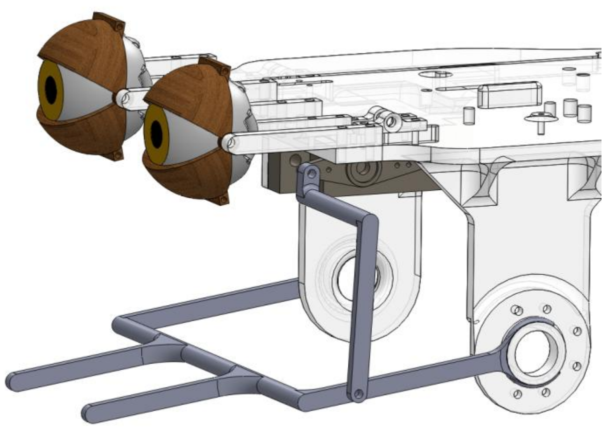

Figure 48: Second Spiral Jaw Mechanism

The final mechanical assembly achieved at the completion of the second design spiral is shown below in Figure 49.

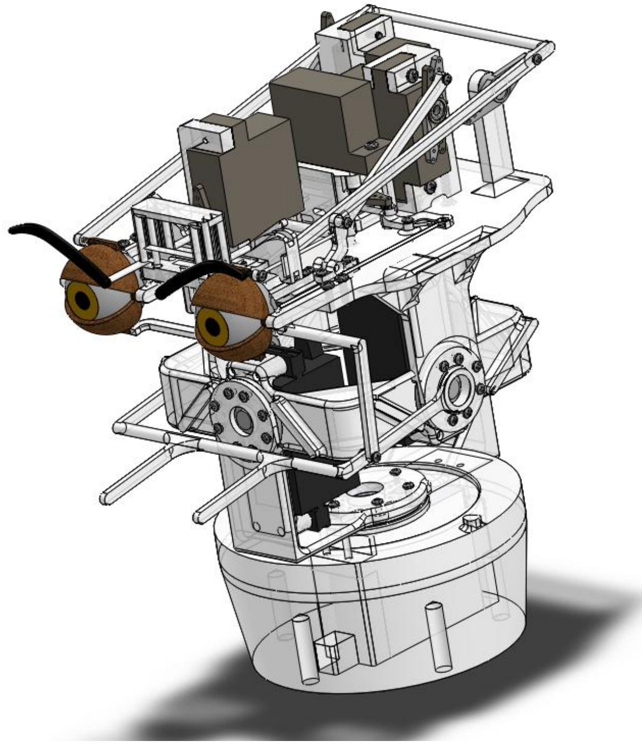

Figure 49: Final Design at Completion of Second Spiral

3: Software

Two types of software were implemented during the course of the project. First, face-tracking software was used to obtain data from a human subject performing a sequence of movements in front of a webcam. The second type was the software that both interpreted the motions recorded by the face-tracking software and implemented it on the robot to create motion.

3.1. Face-Tracking Software

From the start, the goal of this project was to implement face-tracking control for the robot in a pre-recorded playback format. After researching the available commercial software available, such as FaceAPI, it was deemed necessary to investigate free, open-source software that was available based on the high price needed for each of the commercial options.

Since the pursuit was in the direction of open-source software, there were more available options when compared to the commercial options, however they were still very much limited. It was clear from the beginning that there would be no open-source software available to control the robot's eyebrows, eyelids, or mouth. The commercial version of FaceAPI was the only piece of software that could collect data on every degree of freedom. However, all three of these components were simple open-close mechanism in the case of the eyelids and the mouth, and the eyebrows were a simple gradation of vertical positions. These were decided to be hand programmed, while the neck pitch, roll and yaw positions and the eye pitch and yaw positions would be programmed using face-tracking software. The open-source and demo software that was decided on is detailed in the following sections.

3.1.1. FaceAPI Demo In Conjunction with FaceAPI Streaming

To measure the head rotations of the human actors, the demo version of FaceAPI was used, which in the demo state only tracks neck roll, pitch and yaw. An additional open-source software, FaceAPIStreaming, was needed in order to retrieve the data points being measured by the FaceAPI demo. The FaceAPI window and the resulting data are shown below in Figure 50

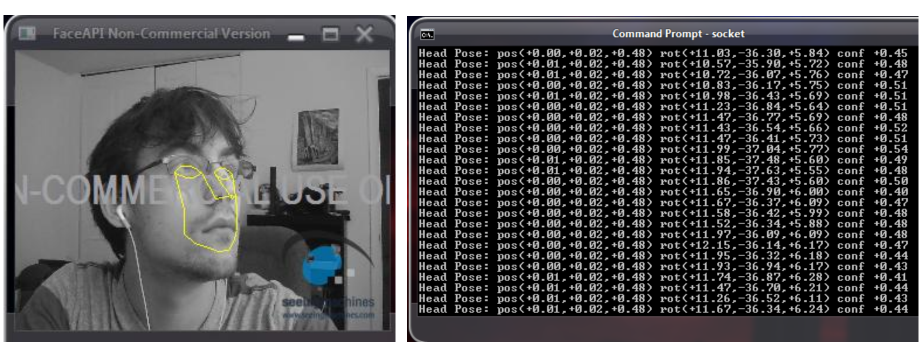

(a) (b)

Figure 50: (a) FaceAPI Demo Window and (b) FaceAPIStreaming Receiving Data

The data output by the FaceAPI demo and FaceAPIStreaming was recorded in the string form similar to:

Head Pose: pos(+0.01,+0.01,+0.41) rot(-15.83,-19.97,+8.72) conf +0.22

The only data needed in this string is "-15.83,-19.97,+8.72" which dictates the necessary rotation of the head for each given time step. The rest of the information could be discarded.

The document with the data was then passed through a MATLAB program that eliminated all of the extraneous information and output the following values: -15.83 degrees for pitch, -19/97 degrees for yaw and 8.72 degrees for roll. The next step in the program was to have MATLAB add 90 degrees to each measurement since the starting value of each servo is 90 degrees, and a negative or positive rotation would add on to the zeroed position. The MATLAB program ends by providing the output of servo pulse values, where in this case they would be: 105 for the pitch position, 99 for the yaw position, and 139 for the roll position.

3.1.2. GazeTracker

GazeTracker is an open-source eye tracking software that outputs data in terms of the current pixel being looked at on a computer screen, since this is intended for use with gaze studies and not mapping eye rotations to a robot. However, with a few adjustments, the eye rotations were extracted from the pixel information. A screenshot of the program interface is shown below in Figure 51.

Figure 51: GazeTracker Interface

GazeTracker required that the camera being used was an infrared camera. Without having the necessary camera technology, a piece of over-developed film was taped over the webcam and a simple circuit with two bright Infrared LEDs, two resistors, and a D cell battery in order to create an infrared camera and an infrared light source.

Since GazeTracker output data in terms of the location of the screen pixel that is being looked at each given time step, the algorithm for mapping pupil position to screen targest spelled out by Hale (2010) was used to convert these screen positions to eye rotations. Once the eye rotations are calculated using the pixel position on the screen in a MATLAB program, they are then transitioned into eye pitch and eye yaw positions in a similar manner as was used with the FaceAPI data in the previous section.

The neck and eye data are then fed into the software package that is used to actuate the robot. The software interprets the servo pulse values and the time stamps for each data point in order to create a performance routine for the robot.

3.2. Actuation Software

During research, a commercial software package called Visual Show Automation (VSA), sold by Brookshire Software LLC, was found that had been produced with the intention of being used for animatronics. This software allowed the user to input servo pulse values along with their timestamps and create performance routines, as previously stated. Figure 52 below depicts an example program that was created in VSA using servo positions and a voice audio file.

Figure 52: Visual Show Automation Routine

VSA simplified the process of syncing motor motions, desired durations of the movements, and the corresponding audio that is associated with the routine.

4: Electrical Hardware

The electrical hardware was dictated mostly by the requirements of software and investigation into other similar systems mentioned. Visual Show Automation is compatible with a list of motor controllers and single board computers. As such, the electrical hardware section will focus on the motor controller that was decided on, the single board computer that was decided on, and the power that is supplied to each of them. Lastly, the schematic of the electrical system is included.

4.1. Motor Controller

The motor controller decided on was the Mini SSCII from Scott Edwards Electronics. The decision was made because it was compatible with VSA, because it was a complete package with not extra assembly required, and it was ready to use straight out of the box. Since this researcher had limited knowledge in the realm of electrical engineering, it was an important requirement for the motor controller to work from the start.

4.2. Single Board Computer

Even though the motor controller could be sent commands from the laptop, it did not seem useful for the robot to be tethered during its operation. A single board computer was pursued so that the robot could operate wherever without needing to constantly have a laptop by its side. Brookshire Software LLC sells a single board computer that is the only option available that is compatible with VSA. As such, the RAPU 5.0 was the only pursuable option. The performance of the board has not made the lack of options a negative though, which is a good thing. Additionally, the it-will-work-right-out-of-the-box application of the RAPU 5.0 was a valuable asset to using this single board computer.

4.3. Power Supply

Three different power supplies were needed, however the RAPU came with its own and did not need additional pursuit. The motor controller calls for 9V input to power the motor controller board itself and 6V input directly to the bank of leads that the servo motors connect to. A 9V battery was used to power the motor controller and four D cell batteries were connected in parallel to power the servo motors.

4.4. System Schematic

The electrical system schematic is depicted below in Figure 53, and the physical system is shown in Figure 54.

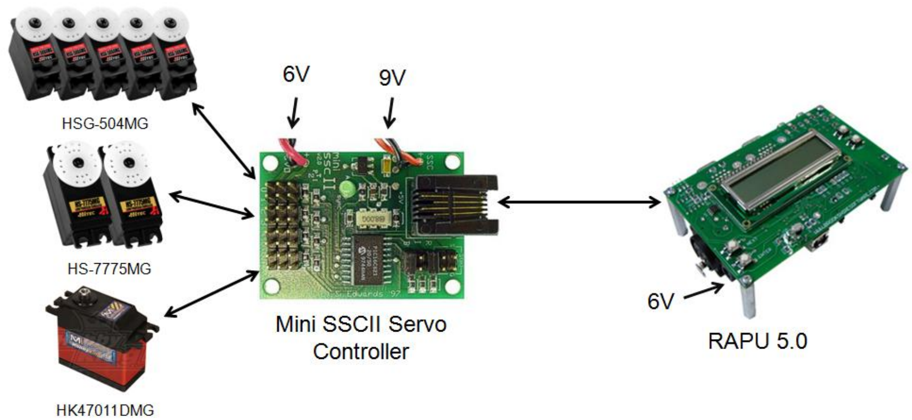

Figure 53: Electrical System Schematic

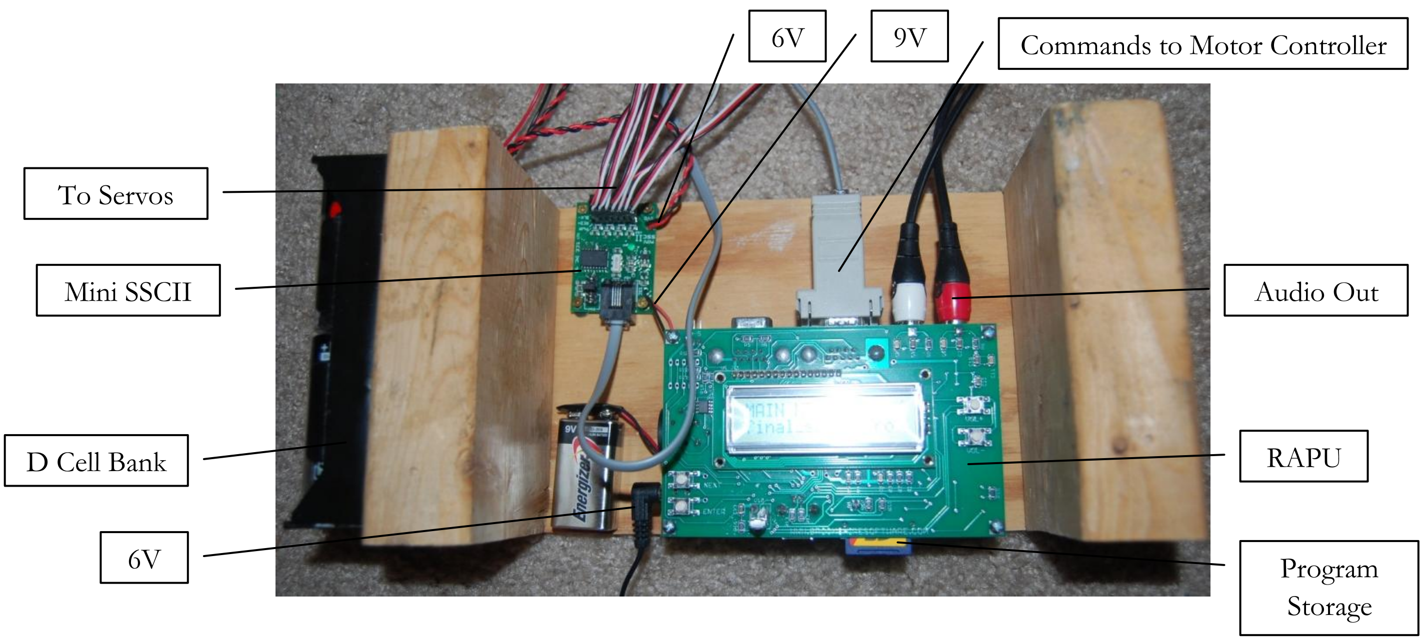

Figure 54: Physical Electrical System

5: Results

The final robot is shown in Figure 55 below with the fiberglass shell both off and on.

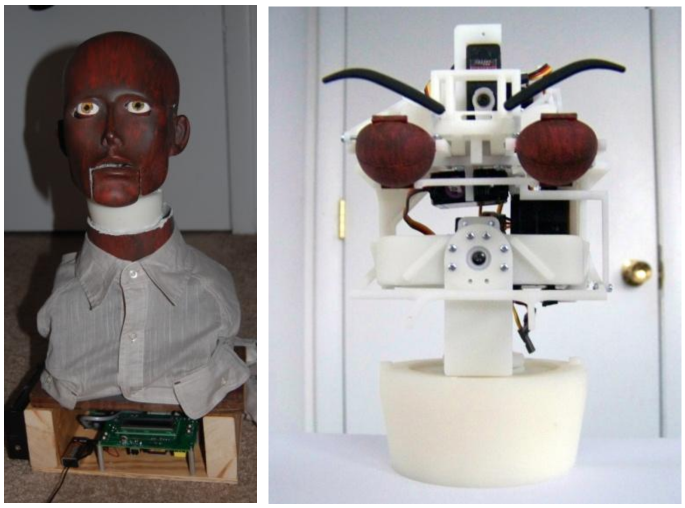

Figure 55: Final Robot

A short video of the robot functioning is located at online at http://www.youtube.com/watch?v=nLD8f7VFyHE. The voice used for the robot is British English, Brian from IVONA text to speech. Even though the video is only of the robot operating for fifteen seconds, the video is proof-of-concept that the robot can operate over a period of time and that period of time is can be lengthened ad infinitum based on the requirements of the program. The proof-of-concept is scalable in regards to the duration of the performance.

It would be beneficial to start with the systems that worked well first, then branch out from there. Very few components caused no issues, however the electrical system worked without a flaw. There was an issue early on where the RAPU and the Mini SSCII were not communicating to each other, but this was because they had two different baud rates. As soon as the baud rates were synchronized at 2400, everything worked perfectly within the electrical system.

The software system came with a few more issues. VSA worked almost perfectly, there was no complaint with this portion of the software. Both open-source face-tracking programs were not precise on their measurements, but that was to be expected through free software and data smoothing algorithms could be implemented in the future to ensure smooth motions during operation. The issue with the face-tracking software was that both programs recorded data at different frequencies which did not match up with the frame rate of VSA at 30 frames per second. The data couldn't be adjusted to match the frequency of VSA, which led to the motions lagging behind the actual motion that had been performed by the actor. To adjust for this, the researcher was forced to truncate and eliminate the data sets in order to try to match the motions back up with the audio file. A prediction algorithm could be implemented in this case in order to calculate what the position of each measured degree of freedom would be for each frame in VSA given the data acquired before the desired time position. All in all, though, this project proved that an animatronic robot could be controlled with open-source software. An additional way to improve the data and potentially the data acquisition frequency would be to purchase the commercial version of FaceAPI, which measures all of the necessary degrees of freedom with an accuracy that is more desirable than that in the demo version.

The main issues that hindered the final result were those discovered during testing the mechanical system. It was quickly discovered that working with fragile, small components lead to breakages if care isn't taken. Parts were broken during the installation due to over-forceful insertions, incorrect alignments, and so on. The two biggest issues that arose and were unable to be corrected in the timeframe of the project were that the eyelids and eyeballs were not perfectly aligned, which led to binding mechanisms, and the improper tolerancing of the key on the rod that connects the left eye yaw mechanism to the right eye pitching mechanism, which also leads to the binding of the mechanism.

Due to both of these bindings, the eyes and eyelids were unable to travel their full range of motion. The eyes and eyelids were still able to move a few degrees in every direction, however pushing the limits past those few degrees led to jammed mechanisms that would have broken if more force was applied by the motors. Each component that was binding in the assembly was filed down to provide more room for movement, however this only provided a few more degrees of motion. These bindings were caused by the imperfect alignment of components. Both the eyes and eyelids are supported by cantilevered beams, which are bent slightly under the force of gravity. This bends would create forces on the eyes and eyebrows which were not designed to be there, which would cause the binding. The eye yaw mechanism is binding because the force is being transferred into the motor mount, instead of the connection rod as was intended. This can be addressed by redesigning the motor mount to have stronger and thicker attachment supports.

A major issue at the end of the project was not having the time available to implement the eyebrow subassembly. Figure 55 depicts the robot with the fiberglass shell on without the eyebrows and the robot without the shell on with eyebrows because the stalks the eyebrows were mounted on were too short to protrude properly from the fiberglass head. More time would have been needed to purchase corrected parts. And if the parts had arrived on time, there would have needed to have been more time to cut the vertical tracks in the fiberglass face needed for the eyebrows to travel as well as time needed to program the eyebrows.

A last minor issue in the mechanical system was the fiberglass shell, it was difficult to machine and collided with the neck as soon as the robot was in motion. As such, the fiberglass needed to be trimmed away in order to ensure movement, which led to a robot that didn't look as much like the concept image created at the start. However, this is a minor issue in relation to the whole robotic system. All of these issues mentioned will be addressed in the future work of this project.

6: Conclusions

While the robot moves according to data achieved from face-tracking software, the binding issues in the mechanical eye and eyelid systems are limitations that prevent the robot from reaching its full potential. Additionally, the availability of open-source software is a limitation that was not expected at the start. The ability to only control neck and eye motion was a limitation on the test of the concept. However, as mentioned before, the commercial version of FaceAPI has the potential to be useful towards recording data for all degrees of freedom from the actor.

The future work for this project is extensive. First, the eyes and eyelids will be redesigned such that they no longer bind and move freely as intended. Second, the eyebrow mechanism will be designed so that it can be implemented on the robot on programmed. Third, smoothing and prediction algorithms will be applied to the face-tracking data in order to ensure smooth motion and timely motion in regards to the VSA frame rate. Fourth, a method will be looked into that blends the neck in with the head (no more gap between the fiberglass neck and the fiberglass head) such that the robot is aesthetically pleasing. Lastly, the remaining aesthetic touches, such as the hat and glasses, will be added to the robot to complete the character. As previously mentioned, this list is extensive, however then end result will be worth it once everything functions properly.

7: Bibliography

Chandler, D. L. (2008, April 9). *Meet Nexi, the Media Lab's latest robot and Internet star*. Retrieved from MIT News: http://web.mit.edu/newsoffice/2008/nexi-0409.html

Dijkstra, P. U., Hof, A. L., Stegenga, B., & De Bont, L. G. (1999). Influence of mandibular length on mouth opening. *Journal of Oral Rehabilitation*, 117-122.

Hale, J. (2010, October 21). *Mapping Pupil Position to Screen Targets*. Retrieved from JJHale.com: http://blog.jjhale.com/2010/10/21/mapping-pupil-position-to-screen-targets/

Hanson Robotics. (2009). *We Bring Robots to Life*. Retrieved from Hanson Robotics: https://hansonrobotics.wordpress.com/

Jung, M., & Sclafani, A. P. (2010). Desired position, shape, and dynamic range of the normal adult eyebrow. *Archives of Facial Plastic Surgery*, 125-127.

Lefohn, A., Caruso, R., Reinhard, E., & Budge, B. (2003). An Ocularist's Approach to Human Iris Synthesis. *IEEE COmputer Graphis and Applications*.

Quesada, V. (2009). *About the Alexander Technique*. Retrieved October 7, 2011, from Alexander Technique: http://alextechniquevictoria.com/about_the_alexander_technique

Robin, S. (2011, May 5). *Human Eye Pupil Types*. Retrieved September 28, 2011, from LiveStrong.com: http://www.livestrong.com/article/63809-human-eye-pupil-types/

(1997). Sensory Reception. In *Encyclopedia Britannic Macropedia.* Britannica Inc.

Stephens, K. (2011, March 15). *Normal Neck Range of Motion*. Retrieved October 15, 2011, from LiveStrong.com: http://www.livestrong.com/article/95456-normal-neck-range-motion/

Tamler, E., Marg, E., Jampolsky, A., & Nawratzki, I. (1959). Electromyography of Human Saccadic Eye Movements. *A.M.A. Archives of Ophthalmology*, 657-661.